

# Estimating Specific Cutting Constants via First Harmonic Force Components in Conventional End Milling Operations

Charles Ming Zheng\* and Kadirikota Rajesh Babu\*\*

**Keywords :** milling, first harmonic force, cutting constants, LGCC.

## ABSTRACT

Charge seepage in piezoelectric sensor often causes a zero-drift problem in measuring cutting force, which can influence the ability to get accurate cutting forces and cutting constants to monitor milling process with a long duration. To overcome this difficulty, a robust method for extracting cutting constants at any moment in milling by only using the measured first harmonic force components is presented. There are two steps in this method for estimating cutting constants. The first is to find the approximations of cutting constants from the ratio of the measured first harmonic force components, and the second utilizes the equations from the components of magnitude of first harmonic force as well as the approximations of cutting constants calculated in the first step to obtain the refined cutting constants by least square method. This paper also discusses the limitations of presented method. The validity of the proposed method is confirmed through milling experiments.

## INTRODUCTION

Milling is a manufacturing process used in a wide range of applications, such as automotive parts, aerospace parts, textile machinery parts and electronic parts. The current trend of "Industry 4.0" requires that manufacturing technology is improved by the introduction of methods including self-optimization, self-configuration and the other intelligent supports in

*Paper Received August, 2018. Revised October, 2019. Accepted December, 2019. Author for Correspondence: Charles Ming Zheng.*

\* Associate Professor, School of Mechanical & Automotive Engineering, Fujian University of Technology, Fuzhou, Fujian 350118, China.

\*\* Associate Professor, Department of Mechanical Engineering, Sri Venkateswara University College of Engineering, Tirupati, A.P 517502, India.

the milling process. Undoubtedly, the cutting force signal can be fundamental and important manufacturing information for the required intelligent milling technology of "Industry 4.0". In the past research, many manufacturing technologies based on cutting force model such as detecting cutter runout, sensing cutting tool breakage and tool wear (Wang, 2003; Altintas, 1989; Zhang, 2010) as well as the prediction of surface location errors and stability in the milling process (Schmitz, 2006; Zheng, 2013) have been developed. The successful operation of the manufacturing technology based on cutting force model depends on the timely feedback of cutting force signal. Therefore, in order to provide intelligent milling technology, the availability of online cutting coefficients or cutting constants in milling process is essential. The type of cutting coefficients or cutting constants depends on the selection of a local cutting force model. Wang and Zheng (2002) organized the local cutting force models into four categories: LVCC (lumped variable cutting coefficients), LGCC (lumped global cutting constants), DVCC (dual-mechanism variable cutting coefficients) and DGCC (dual-mechanism global cutting constants). The LVCC and DVCC differ from LGCC and DGCC in the shearing coefficients which vary with cutting parameters instead of being global constants. On the other hand, the DVCC and DGCC separate ploughing force from shearing force and have double number cutting coefficients/constants comparing with the LVCC and LGCC. In order to obtain the predictable cutting coefficients/constants, most cutting coefficients/constants are expressed as function of chip thickness or average chip thickness (Kline, 1982; Wang, 1994; Zhang, 2005). Some cutting coefficients/constants are established as functions of chip thickness, axial depth of cut and cutting geometry (Yang, 1991; Feng, 1994; Pan, 2017). However, the calibrated coefficients/constants cannot satisfy the requirements of self-optimization, self-configuration and self-diagnosis in intelligent milling technology such as the application of self-diagnosis of cutting tool wear. For the purpose of self-diagnosis of cutting tool wear, the cutting coefficients/constants need to be identified at any

instant in milling process. Once the threshold value of cutting coefficients/constants is detected, the worn cutting tool can be replaced automatically, and the chip thickness dependent coefficients/constants are no longer useful for a self-diagnosis of cutting tool wear. Earlier works on the online identification of the dual-mechanism global cutting constants have been presented by Wang et al. (2003, 2004). Based on the analytical nature of frequency milling force model, three methods were presented in their works. The first method makes use of the first harmonic milling force components, the second method uses average milling forces and the ratio of the first harmonic force components, and the third method utilizes the first harmonic milling force components and the ratios of first harmonic force components and second harmonic force components. Although dual-mechanism global cutting constants has advantages in independence of chip thickness and better accuracy in predicting cutting force, the model of lumped global cutting constants (LGCC) is still popular for the industry and academia due to its simplicity in developing cutting force model. Previous works have shown that LGCC can be identified from the measured average forces and estimated online from the average forces of a single cutting test (Wang, 2004; Zhang, 2005). However, charge leakage in piezoelectric sensor often causes the average forces to drift with time (Zhang, 2005). The identification of lumped global cutting constants based on average forces model is not suitable for applications wherein continuous monitoring of milling process is desirable. To overcome a zero drift problem due to the charge leakage in piezoelectric dynamometer, it is necessary to identify the lumped global cutting constants online without inclusion of the measured average force, which forms the crux/objective of the present research study.

Section 2 of this paper first presents a method to find the approximations of LGCC from the analytical expressions for the first harmonic force components based on the assumption that cutting constants are real numbers. Section 3 deals with the method of obtaining optimal LGCC by truncated Taylor's series that utilizes expressions of magnitudes of first harmonic force components as well as the approximation of cutting constants. Numerical and experimental verifications are presented in Section 4 followed by conclusions.

### EXTRACTING LGCC WITH RATIO OF THE FIRST HARMONIC FORCE COMPONENTS

Based on the work by Wang et al. (1994), a frequency milling force model with LGCC was developed, and the vector of total milling forces can

be expressed as a function of cutter angular displacement by

$$\mathbf{f}(\phi) = \begin{bmatrix} f_x(\phi) \\ f_y(\phi) \end{bmatrix} = \sum_{k=-\infty}^{\infty} \mathbf{A}[Nk] e^{jNk\phi}, \quad (1)$$

where

$$\mathbf{A}[Nk] = \begin{bmatrix} A_x[Nk] \\ A_y[Nk] \end{bmatrix} = \frac{Nk t_x}{2\pi} \begin{bmatrix} 1 & k_r \\ -k_r & 1 \end{bmatrix} \begin{bmatrix} CP_1[Nk] \\ CP_2[Nk] \end{bmatrix}, \quad (2)$$

are the coefficients of the Fourier series expansion of total milling forces in X and Y directions. It is shown that the spectra magnitude of total milling forces at normalized harmonic frequencies  $Nk$  can be expressed explicitly as the algebraic functions of cutting parameters.  $k_t$  and  $k_r$  denote as LGCC in tangential and radial directions. They can be shown from Equation (2) that

$$\begin{pmatrix} k_t \\ k_r \end{pmatrix} = \begin{bmatrix} CP_1[Nk] & CP_2[Nk] \\ CP_2[Nk] & -CP_1[Nk] \end{bmatrix}^{-1} \begin{pmatrix} A_x[Nk] \\ A_y[Nk] \end{pmatrix} \frac{2\pi}{Nt_x}, \quad (3)$$

where  $N$  and  $t_x$  denote as flute number of cutter and feed per tooth. Cutting parameter functions  $CP_1$  and  $CP_2$  are expressed in terms of flute number of cutter  $N$ , helix angle  $\alpha$ , radius of cutter  $R$ , axial depth of cut  $d_a$ , entry cutting angle  $\theta_1$  and exit cutting angle  $\theta_2$  by

$$\begin{pmatrix} CP_1[Nk] \\ CP_2[Nk] \end{pmatrix} = CWD[Nk] \begin{pmatrix} P_1[Nk] \\ P_2[Nk] \end{pmatrix}, \quad (4)$$

with

$$CWD[Nk] = \frac{2R \sin \frac{Nk}{N/\eta_a} \pi}{Nk \tan \alpha} e^{-j \frac{Nk}{N/\eta_a} \pi}, \eta_a = \frac{Nd_a \tan \alpha}{2\pi R}, \quad (5)$$

$$\begin{pmatrix} P_1[Nk] \\ P_2[Nk] \end{pmatrix} = \begin{bmatrix} \frac{e^{-jNk\theta_2}}{2[4-(Nk)^2]} (jNk \sin 2\theta_2 + 2 \cos 2\theta_2) \\ \frac{e^{-jNk\theta_2}}{2[4-(Nk)^2]} (jNk \cos 2\theta_2 - 2 \sin 2\theta_2) - \frac{e^{-jNk\theta_2}}{2jNk} \end{bmatrix} - \begin{bmatrix} \frac{e^{-jNk\theta_1}}{2[4-(Nk)^2]} (jNk \sin 2\theta_1 + 2 \cos 2\theta_1) \\ \frac{e^{-jNk\theta_1}}{2[4-(Nk)^2]} (jNk \cos 2\theta_1 - 2 \sin 2\theta_1) - \frac{e^{-jNk\theta_1}}{2jNk} \end{bmatrix} = \begin{bmatrix} \frac{e^{-jNk\theta}}{2[4-(Nk)^2]} (jNk \sin 2\theta + 2 \cos 2\theta) \\ \frac{e^{-jNk\theta}}{2[4-(Nk)^2]} (jNk \cos 2\theta - 2 \sin 2\theta) - \frac{e^{-jNk\theta}}{2jNk} \end{bmatrix}_{\theta_1}^{\theta_2}. \quad (6)$$

Equation (3) shows that LGCC may be determined from the measured force at different harmonic frequencies in a single cutting test. When the normalized harmonic frequency  $Nk=0$  is selected, it means that measured average forces are used to estimate the LGCC. When it is desirous to extract LGCC without the knowledge of average forces, force measurements at harmonic frequencies may aid the operator/user to identify LGCC through online. For the acquisition of highest signal to noise ratio, the measured first harmonic force components ( $N$  or  $-N$ ) seems to be more suitable to use in extracting the cutting constants rather than other harmonic force components. Comparing with usefulness of measured

average forces, it is worth noticing that Eq. (3) may not be applied directly for extracting cutting constants by using the measured first harmonic force components due to the lack of knowledge of starting angular position of the measurement with respect to the force model coordinate system. This implies that in order to use  $k$ th ( $k \neq 0$ ) harmonic force component to identify cutting constants via Eq. (3), the Fourier coefficients  $\mathbf{A}[Nk]$  in Eq. (3) should be transformed from the measured harmonic force components  $\mathbf{A}'[Nk]$  through following transformation:

$$\mathbf{A}[Nk] = \mathbf{A}'[Nk]e^{-jNk\Delta\phi}$$

or 
$$\begin{pmatrix} A_x[Nk] \\ A_y[Nk] \end{pmatrix} = \begin{pmatrix} A'_x[Nk] \\ A'_y[Nk] \end{pmatrix} e^{-jNk\Delta\phi}, \quad (7)$$

where  $\Delta\phi$  denote as the phase angle difference between the starting angular position of the force measurement and the origin of cutting position defined by the force model as shown in Figure 1.

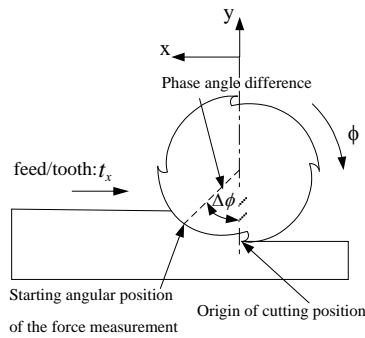


Fig. 1 Phase angle difference between the starting angular position of the force measurement and the origin of cutting position.

The phase angle difference can be calibrated by an angular position sensor. However, even if the milling machine is equipped with an angular position sensor; the starting angular position of the force measurement is still difficult to align with the origin of force model coordinate system. An extracting LGCC method using the measured first harmonic force component without the knowledge of phase angle difference is presented here. By setting  $k=1$  in Equation (7), the ratio of first harmonic forces can be expressed as

$$\frac{A_x[N]}{A_y[N]} = \frac{A'_x[N]e^{-jN\Delta\phi}}{A'_y[N]e^{-jN\Delta\phi}} = \frac{A'_x[N]}{A'_y[N]} = b + jc. \quad (8)$$

Equation (8) shows that the phase angle difference between the first harmonic force components in X and Y directions remain the same regardless of the starting angular position of the force measurement, and the values of  $b$  and  $c$  can be obtained from the force measurement. According to the expression of Eq. (2), left hand side of Eq. (8) can be written as

$$\frac{A_x[N]}{A_y[N]} = \frac{P_1[N] + k_r P_2[N]}{-k_r P_1[N] + P_2[N]}. \quad (9)$$

Equating both right hand sides of the Eq. (8) and Eq. (9) results in the following equation:

$$\frac{P_1(N) + k_r P_2(N)}{-k_r P_1(N) + P_2(N)} = \frac{(P_{1R} + jP_{1I}) + k_r(P_{2R} + jP_{2I})}{-k_r(P_{1R} + jP_{1I}) + (P_{2R} + jP_{2I})} = b + jc. \quad (10)$$

where  $P_{1R}, P_{2R}, P_{1I}, P_{2I}$  are the real and imaginary parts of  $P_1(N)$  and  $P_2(N)$ , respectively. Based on the assumption in which cutting constants are real numbers and splitting both sides of Equation (10) into their real and imaginary parts, two possible values of  $k_r$  can be solved with

$$k_{r1} = \frac{bP_{2R} - cP_{2I} - P_{1R}}{bP_{1R} - cP_{1I} + P_{2R}}, k_{r2} = \frac{bP_{2I} + cP_{2R} - P_{1I}}{bP_{1I} + cP_{1R} + P_{2I}}. \quad (11)$$

Substituting  $k_{r1}$  into Eq. (2) and using the magnitude components of first harmonic forces in X and Y directions, two possible values of  $k_t$  can be also determined by the following formula:

$$k_{t1} = \frac{2\pi|A_x[N]|}{Nt_x|CP_1[N] + k_{r1}CP_2[N]}, k_{t2} = \frac{2\pi|A_y[N]|}{Nt_x|-k_{r1}CP_1[N] + CP_2[N]}. \quad (12)$$

It is noteworthy to observe that the magnitude components of first harmonic forces will remain unchanged regardless of the phase angle difference. Therefore, Equation (12) can be rewritten as

$$k_{t1} = \frac{2\pi|A'_x[N]|}{Nt_x|CP_1[N] + k_{r1}CP_2[N]}, k_{t2} = \frac{2\pi|A'_y[N]|}{Nt_x|-k_{r1}CP_1[N] + CP_2[N]}. \quad (13)$$

Similarly, substituting  $k_{r2}$  into Eq. (2) and using the magnitude of first harmonic forces in X and Y directions, there also exists two possible values of  $k_t$ . In that case, they become:

$$k_{t3} = \frac{2\pi|A'_x[N]|}{Nt_x|CP_1[N] + k_{r2}CP_2[N]}, k_{t4} = \frac{2\pi|A'_y[N]|}{Nt_x|-k_{r2}CP_1[N] + CP_2[N]}. \quad (14)$$

According to the above analysis, four sets of possible cutting constants can be obtained from the first harmonic forces. They are  $(k_{r1}, k_{t1})$ ,  $(k_{r1}, k_{t2})$ ,  $(k_{r2}, k_{t3})$  and  $(k_{r2}, k_{t4})$ . In theory, if the measured first harmonic forces do not include ploughing force components, it can be found that  $(k_{r1}, k_{t1}) = (k_{r1}, k_{t2}) = (k_{r2}, k_{t3}) = (k_{r2}, k_{t4})$ . However, in most cutting conditions, shearing and ploughing forces are all associated with the first harmonic forces. Thus, the four sets of possible solutions are different in practical milling operations. From the four sets of possible cutting constants, the best set of the possible cutting constants can be determined by finding the set of cutting constants with minimum error of predicting forces by following equations:

$$A_{\min} = \min[A^{(i,j)}], \begin{cases} \text{when } i=1, & j=1,2 \\ \text{when } i=2, & j=3,4 \end{cases}, \quad (15)$$

$$= \min\left\{\left|A'_x[N]\right| - \left|A_x^{(i,j)}[N]\right|\right\}^2 + \left\{\left|A'_y[N]\right| - \left|A_y^{(i,j)}[N]\right|\right\}^2$$

$$\begin{pmatrix} A_x^{(i,j)}[N] \\ A_y^{(i,j)}[N] \end{pmatrix} = \frac{Nk_{ij}t_x}{2\pi} \begin{bmatrix} 1 & k_{ri} \\ -k_{ri} & 1 \end{bmatrix} \begin{pmatrix} CP_1[N] \\ CP_2[N] \end{pmatrix}. \quad (16)$$

In Equation (15), the best set of the possible cutting constants would be taken up by finding the cutting constants  $(k_{ri}, k_{ij})$  corresponding to the minimum value of the sum of squared residuals,  $A_{\min}$ .

The cutting constants  $(k_{ri}, k_{ij})$  corresponding to  $A_{\min}$  are referred to quasi-available cutting constants,  $(k_{rq}, k_{iq})$  in this paper. It is noted that the quasi-available cutting constants may be unable to predict the cutting force optimally. To improve the quasi-available cutting constants, a refining procedure is presented in next section.

### REFINING QUASI-AVAILABLE CUTTING CONSTANTS

A non-linear least square method is used here to refine the quasi-available cutting constants by successive iterations. From Eq. (2), the first harmonic force components can be written as

$$\begin{pmatrix} A_x[N] \\ A_y[N] \end{pmatrix} = \begin{bmatrix} CP_1[N] & CP_2[N] \\ CP_2[N] & -CP_1[N] \end{bmatrix} \begin{pmatrix} k_1 \\ k_2 \end{pmatrix}, \quad (17)$$

where

$$\begin{pmatrix} k_1 \\ k_2 \end{pmatrix} = \frac{Nt_x}{2\pi} \begin{pmatrix} k_t \\ k_r \end{pmatrix} = \mathbf{k}. \quad (18)$$

It is desired to find the vector  $\mathbf{k}$  of cutting constants such that the values of  $(|A_x[N]|^2, |A_y[N]|^2)$  fit well into the force measurements,  $(|A'_x[N]|^2, |A'_y[N]|^2)$  in the least square sense. The detailed process for finding the optimal cutting constants can be found in the appendix.

A flowchart is presented in Figure 2 for finding the optimal cutting constants  $k_{rd}$  and  $k_{ld}$ . The procedure starts with finding the four sets of possible cutting constants from the ratio of first harmonic forces as shown in Eqs. (11) to (14). The quasi-available cutting constants can serve as the initial values of  $\mathbf{k}^{(0)}$  vector to find the optimal cutting constants  $k_{rd}$  and  $k_{ld}$  through an iteration analysis based on a non-linear least square method. It is noted that the initial values of  $\mathbf{k}^{(0)}$  vector are close enough to the desired  $\mathbf{k}$  vector in most cutting conditions, and thus the iteration procedure requires only a small number of iterations to be expected.

### MODEL VERIFICATION AND DISCUSSIONS

#### Identifying LGCC from Lumped Shearing Force

The verification starts by specifying the lumped global cutting constants (LGCC) as shown in Table 1 to simulate the total milling forces.

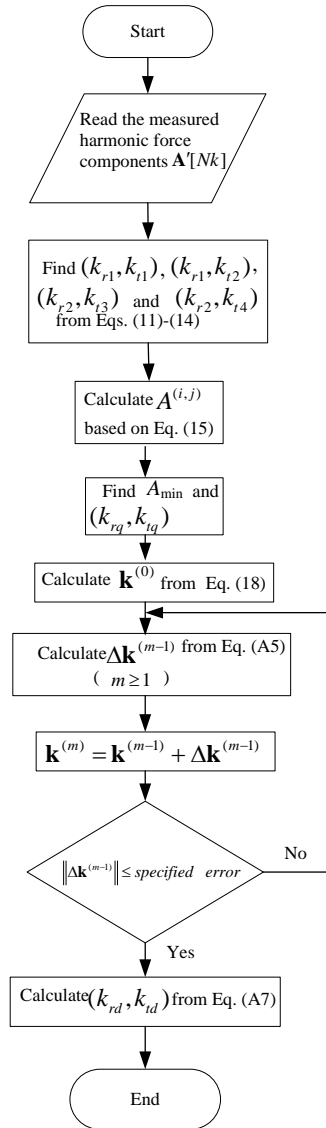


Fig. 2 Flow chart for finding optimal cutting constants.

Table 1. The cutting conditions for the identification of cutting constants in the numerical simulation.  $R = 5 \text{ mm}$ ,  $\alpha = 30^\circ$ ,  $t_x = 0.025 \text{ mm/tooth}$ .

No.	$\theta_1$ (deg)	$\theta_2$ (deg)	$d_a$ (mm)	N
1	150	180	4	4
2	90	180	6	4
3	0	90	5	4
4	0	30	3	3
5	0	179.99	5.5	3
6	45	135	7.5	3
7	0	179.99	4.2	4
8	0	90	6.8	8

Using the numerical integration method presented by Kline et al. (1982) to emulate the cutting force, then the cutting constants  $(k_{r1}, k_{t1})$ ,  $(k_{r1}, k_{t2})$ ,  $(k_{r2}, k_{t3})$  and  $(k_{r2}, k_{t4})$  are identified from the simulated first harmonic forces through Eqs. (11) to (14). In addition, by letting  $k=0$ , Eq. (3) can be rewritten as:

$$\begin{pmatrix} k_{r0} \\ k_{t0}, k_{r0} \end{pmatrix} = \begin{bmatrix} CP_1[0] & CP_2[0] \\ CP_2[0] & -CP_1[0] \end{bmatrix}^{-1} \begin{pmatrix} A_x[0] \\ A_y[0] \end{pmatrix} \frac{2\pi}{Nt_x}, \quad (19a)$$

or

$$\begin{pmatrix} k_{r0} \\ k_{t0}, k_{r0} \end{pmatrix} = \begin{bmatrix} CP_1[0] & CP_2[0] \\ CP_2[0] & -CP_1[0] \end{bmatrix}^{-1} \begin{pmatrix} A'_x[0] \\ A'_y[0] \end{pmatrix} \frac{2\pi}{Nt_x}. \quad (19b)$$

Equations (19a) and (19b) presented here are similar to the works of Wang et al. (1994). Therefore, the identified cutting constants from Eq. (19b) agree with the works of Wang et al. (1994). The two equations show that if zero-drift problem do not exist in measuring milling forces, the lumped global cutting constants can be simply identified from the measured average cutting forces. It should be emphasized that the average cutting forces can be measured directly regardless of the starting angular position of the force measure, i.e.,  $(A_x[0], A_y[0]) = (A'_x[0], A'_y[0])$ , which is the advantage of using measured average cutting forces to identify cutting constants, comparing with using measured harmonic forces to identify cutting constants. It is noted that the identification of cutting constants from average forces is independent of the use of harmonic forces to identify the cutting constants due to the independent nature at each Fourier coefficients of cutting force. As shown in Table 2, the cutting constants identified from the first harmonic forces ( $k=1$ ) are nearly equal to the specified cutting constants as well as the cutting constants identified from average forces ( $k=0$ ), except the identified cutting constants in last two sets of cutting conditions. In the case No. 7 of cutting conditions, the inaccurate cutting constants identified from first harmonic forces can be explained by that the harmonic force components of X and Y forces do not exist for an end mill with four flutes in slot milling, since  $P_1[Nk]$  and  $P_2[Nk]$  in Eq. (6) are zeros in that case. Further, for an end mill with flute number  $N=4, 6, 8, \dots$ , Eq. (6) shows that only average force components exist in slot milling. The cutting condition listed in No. 7 of Table 1 is close to slot milling ( $\theta_1=0, \theta_2=180^\circ$ ), and thus the cutting constants identified from first harmonic forces are sensitive with calculation error to be expected. Similarly, the harmonic force components of X and Y forces also nearly vanish under cutting conditions No. 8, since the value of  $\eta_a$  is close to 1. As shown in Eq. (5),  $CWD[Nk]$  becomes zero when  $\eta_a$  is a natural number, resulting in the disappearance of

harmonic force components. This condition implies that axial depth of cut  $d_a$  can be written as

$$d_a = \frac{2m\pi R}{N \tan \alpha}, \quad m=1, 2, 3, \dots, \quad (20)$$

where  $m$  is a nature number. As shown in Table 2, except for the above mentioned limitations of cutting conditions, the four sets of possible cutting constants identified from simulated first harmonic forces are identical due to the representation of cutting force by lumped shearing mechanism only. This means that the refining procedure of the cutting constant does not need to be performed. However, in practical milling, the ploughing mechanism have influence on cutting forces and thus the four sets of possible cutting constants identified from Eqs. (11) to (14) would be different.

Table 2. The identified cutting constants from the average forces and the first harmonic forces for the cutting conditions in Table 1. Specified cutting constants  $(k_r, k_t) = (1000MPa, 0.3)$ .

Case No.	Identified LGCC from the average forces (k=0) $k_{r0}$ $k_{t0}(MPa)$	Identified LGCC from the first harmonic forces (k=1)	
		$k_{r1}$ $k_{t1}, k_{t2}(MPa)$	$k_{r2}$ $k_{t3}, k_{t4}(MPa)$
1	0.3	0.3	0.3
	999.7	999.9,999.7	999.9,999.9
2	0.3	0.3	0.3
	1000	1000.5,1000.2	1000,1000.1
3	0.3	0.299	0.3
	1000	1001.2,1000.4	1000,1000
4	0.3	0.3	0.3
	1000.2	1000.3,999.9	1000.3,1000.7
5	0.3	0.3	0.3
	1000	1000,1000	1000,1000
6	0.3	0.3	0.3
	1000	999.9,999.9	1000,999.9
7	0.3	0.3	0.316
	1000	940.7,940.7	940.7,893.7
8	0.3	0.636	0.325
	1000	567.8, 905.3	946.3,913.7

In that case, the quasi-available cutting constants need to be determined in order to find the optimal cutting constants. The validity of refining

procedure for estimating optimal cutting constant as presented in previous section will be verified through milling experiments.

**Experimental Verification**

Milling experiments were carried out to verify of the identification with first harmonic force components for the cutting constants. In the experiments, the cutting constants via first harmonic force components are identified from the measured cutting forces by using the flow chart as shown in Fig. 2, which including the equations proposed by this paper. The cutter/work pair is used: a three-fluted end mill of 10mm diameter with A12024-T4. Based on the cutting conditions listed in Table 3, the cutting forces were measured with the Kistler 9255B dynamometer.

Table 3. The cutting conditions for the identification of cutting constants and the comparing milling forces of predicted and measured results.  $R = 5 \text{ mm}$ ,

$\alpha = 30^\circ$ ,  $N=3$ , dry cutting

Case No.	$d_a$ (mm)	$d_r$ (mm)	Spindle speed (rpm)	Feed rate (mm/min)	Type of milling
1	3	1	900	70	down
2	3	1	900	90	down
3	3	1	900	110	down
4	3	1	900	130	down
5	3	1	500	80	down
6	2.5	2	500	100	down
7	2.5	2	500	120	down
8	2.5	2	300	90	down
9	2.5	2	200	100	up
10	2.5	2	200	120	up
11	2.5	10	400	100	slot
12	3	2	300	120	down

Firstly, the force measurements are operated with a short duration for the cutting conditions from No. 1 to No. 10. Therefore, the measured average forces are reliable in those cases. The cutting constants listed in Table 4 are identified by using the measured average forces ( $k=0$ ) and first harmonic forces ( $k=1$ ), respectively.

As noted, there are some differences among the four sets of possible cutting constants,  $(k_{r1}, k_{t1})$ ,

$(k_{r1}, k_{t2})$ ,  $(k_{r2}, k_{t3})$  and  $(k_{r2}, k_{t4})$  as shown in Table 4.

Table 4. The identified cutting constants form the average forces and the first harmonic forces for the cutting conditions in Table 3.

Case No.	LGCC form the average forces (k=0)		LGCC form the first harmonic forces (k=1)		
	$k_{r0}$ $k_{t0}$ (MPa)	$k_{r1}$ $k_{t1}, k_{t2}$ (MPa)	$k_{r2}$ $k_{t1}, k_{t2}$ (MPa)	$k_{r3}$ $k_{t3}$ (MPa)	$k_{r4}$ $k_{t4}$ (MPa)
1	0.686 2570	0.686 2470,2429	0.674 2449,2455	0.674 2455	0.676 2452
2	0.651 2213	0.674 2158,2055	0.637 2108,2122	0.637 2122	0.642 2114
3	0.619 1954	0.658 1928,1789	0.603 1862,1880	0.603 1880	0.609 1869
4	0.594 1799	0.643 1789,1632	0.577 1715,1735	0.577 1735	0.585 1723
5	0.579 1713	0.633 1710,1547	0.561 1635,1655	0.561 1655	0.569 1643
6	0.473 1372	0.414 1225,1319	0.456 1275,1274	0.456 1274	0.455 1274
7	0.452 1293	0.384 1150,1262	0.436 1209,1208	0.436 1208	0.435 1208
8	0.427 1212	0.352 1080,1201	0.412 1142,1140	0.412 1140	0.411 1141
9	0.446 1027	0.61 911,1076	0.379 1032,1066	0.379 1032	0.367 1039
10	0.422 1004	0.59 891,1640	0.368 1006,1037	0.368 1006	0.356 1013
11	0.426 1076	0.282 889,888	0.283 887,888	0.283 887	0.282 887
12	0.545 259	0.323 1017,1136	0.386 1077,1074	0.386 1074	0.384 1076

It can be attributed by the existence of ploughing forces which are not clearly separated from the lumped shearing force model. The optimal cutting constants from first harmonic forces,  $(k_{rd}, k_{td})$ , and the cutting constants identified from the measured average forces,  $(k_{r0}, k_{t0})$ , are used to predict the cutting forces. Some predicted forces in the angle domain and frequency domain are shown in Figs. 3-4 along with the measured forces. Strictly speaking, the simulation results both by using  $(k_{r0}, k_{t0})$  and  $(k_{rd}, k_{td})$  were in agreement with those of predicted forces evaluated with the measured ones. Those identified cutting constants  $(k_{r0}, k_{t0})$  and  $(k_{rd}, k_{td})$  for the cutting conditions as depicted in Table 4 are expressed as functions of average chip thicknesses by

$$\begin{cases} k_{r0} = 0.23(\bar{t}_c)^{-0.22} \\ k_{t0} = 362.13(\bar{t}_c)^{-0.39} \\ k_{rd} = 0.17(\bar{t}_c)^{-0.29} \\ k_{td} = 363.92(\bar{t}_c)^{-0.38} \end{cases} \quad (21)$$

A little prediction errors are found mainly from the existence of cutter runout which is not considered in the presented force model. Based on the work by Wang et al. (2003), the cutter runout related cutting forces are characterized by having harmonic force components at one spindle frequency above and below the nominal cutting force frequencies,  $Nk$ . For example, the measured harmonic forces components at  $f_0, 2f_0, 4f_0, 5f_0 \dots$  ( $f_0$ =spindle frequency=15 Hz) can be attributed to be caused by cutter runout as shown in Fig. 3.

Two additional milling experiments using the same cutter/work pair are conducted with different cutting conditions from cases 11 and 12 of Table 3. According to the prediction results from case of No. 11, the simulation results by using  $(k_{r0}, k_{t0})$  seem to have better predictive accuracy than the simulation results by using  $(k_{rd}, k_{td})$  in angular domain as shown in Fig. 5. In that case, the four sets of possible cutting constants are nearly identical. This result indicates that ploughing forces components practically vanish in the first harmonic forces. Therefore, the cutting constants identified from the first harmonic forces are pure shearing constants instead of lumped shearing constants.

In addition, the cutting constants identified from average forces are obviously larger than the cutting constants identified from the first harmonic forces as shown in Table 4, which implies that the ploughing forces components are still associated with shearing forces components in the average forces contents.

Due to the absence of ploughing forces components in first harmonic forces, the simulation results by using  $(k_{rd}, k_{td})$  fail to predict the average forces components in the case of No. 11. On the other hand, the simulation results seem to be acceptable in predicting the first harmonic forces by using  $(k_{r0}, k_{t0})$ , although the predicted first harmonic forces based on  $(k_{rd}, k_{td})$  are more accurate.

For further verification of the identification method based on first harmonic forces, the force measurement is operated during a longer duration under the No. 12 cutting conditions. Obviously, the cutting constants identified from measured average forces are not reasonable for practical milling, since they fail to predict the measured harmonic cutting forces as shown in Fig. 6. On the other hand, the predicted forces from  $(k_{rd}, k_{td})$  succeed in predicting the milling forces at all nominal cutting frequencies, except for the average forces components. It is also noted that the identified cutting constants are very close to the calibrated cutting constants from Eq. (21). Through experimental results above, the presented identification method of LGCC From first harmonic force components in end milling has been validated.

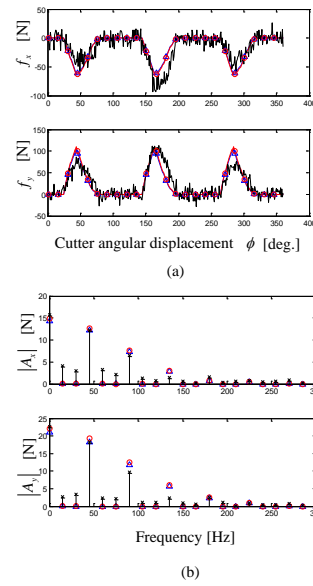


Fig. 3 Comparison of measured and predicted forces, (a): in angle domain and (b): in frequency domain. Solid line: measured forces. O: predicted forces using cutting constants identified from average forces.  $\Delta$ : predicted forces using cutting constants identified from first harmonic forces. Cutting conditions: case 3 in Table 3.

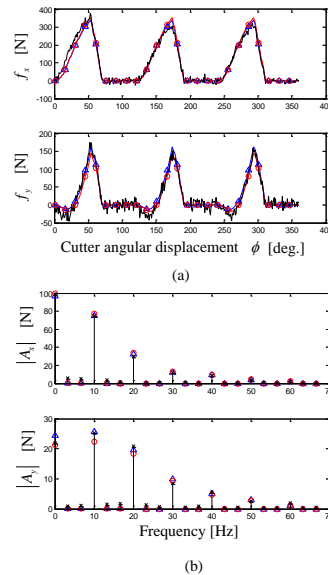


Fig. 4 Comparison of measured and predicted forces, (a): in angle domain and (b): in frequency domain. Solid line: measured forces. O: predicted forces using cutting constants identified from average forces.  $\Delta$ : predicted forces using cutting constants identified from first harmonic forces. Cutting conditions: case 10 in Table 3.

## CONCLUSIONS

Comparing with the existing methods to identify LGCC based on cutting force model, this paper presents a method for extracting cutting constants without the need of measured average cutting forces. Charge seepage in piezoelectric sensor often causes a zero-drift problem in using force dynamometer as shown in Fig. 7, and it will be difficult to get accurate average cutting forces to identify cutting constants for continuous monitoring of milling process with a long duration.

The problem could be solved by the presented method. In this study, by using the ratio of first harmonic forces, four sets of possible cutting constants were found based on the assumption that cutting constants are real numbers. Subsequently, a set of cutting constants is selected from the four sets of possible cutting constants by fitting the measured first harmonic force in the least square sense. Finally, the quasi-available cutting constants can serve as the initial values to find the optimal cutting constants  $k_{rd}$  and  $k_{fd}$  through an iteration analysis based on a non-linear least square method.

The main conclusions extracted from present work are given as follows:

- 1) Strictly speaking, in contrast with the measured cutting forces, the cutting constants as identified from both average forces and first harmonic forces have good prediction accuracy so far as online identification of cutting constants are concerned.
- 2) In theory, if the four sets of possible cutting constants are found to be identical such as in slot milling for a cutter with three flutes, there are no ploughing forces components in the first harmonic forces contents but the ploughing forces components do not vanish in the average force components. In that case, the simulation results seem to be acceptable in predicting the cutting forces by using the cutting constants identified from average forces, although the predicted first harmonic forces based on the optimal cutting constants are more accurate.
- 3) Cutting conditions at or close to some special cases will result in zero or very small values of first harmonic forces and are not allowed in the application of presented method. In addition, in slot milling, first harmonic forces will also vanish for an end mill with 4, 6, 8...cutting flutes and the presented identification method should be avoided to use under these conditions.
- 4) Through the application of the presented identification method, a continuous monitoring of milling process is made possible where the piezoelectric dynamometer suffers from zero-drift problem.

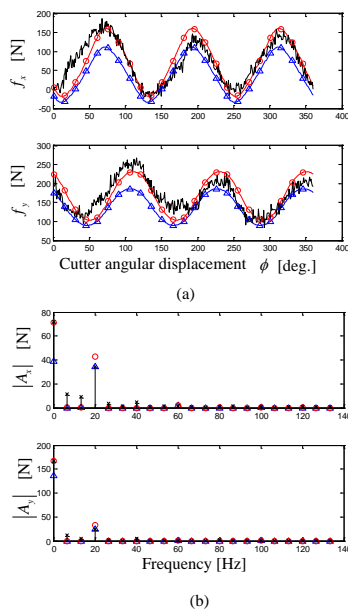


Fig. 5 Comparison of measured and predicted forces, (a): in angle domain and (b): in frequency domain. Solid line: measured forces. O: predicted forces using cutting constants identified from average forces.  $\Delta$ : predicted forces using cutting constants identified from first harmonic forces. Cutting conditions: case 11 in Table 3.

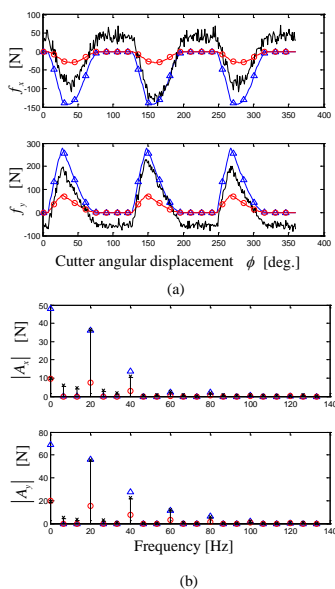


Fig. 6 Comparison of measured and predicted forces, (a): in angle domain and (b): in frequency domain. Solid line: measured forces. O: predicted forces using cutting constants identified from average forces.  $\Delta$ : predicted forces using cutting constants identified from first harmonic forces. Cutting conditions: case 12 in Table 3.

## ACKNOWLEDGEMENT

The authors gratefully acknowledge the financial support from “Guo, Fei-Fei’s Workroom of Mechanical Manufacturing and Automation Specialty” and “Research Center for Intelligent Manufacturing Application” in Quanzhou Vocational and Technical University.

## REFERENCES

- Altintas, Y., Yellowley, I., "In-process detection of tool failure in milling using cutting force models,"; ASME Journal of Engineering for Industry, Vol. 111, pp. 149–157(1989).
- Feng, H., Menq, C., "The prediction of cutting force in ball-end milling process—Part II: Cut geometry analysis and model verification,"; International Journal of Machine Tools & Manufacture, Vol. 34, pp. 711–719(1994).
- Kline, W.A., DeVor, R.E. and Lindberg, J.R., "The Prediction of Cutting Forces in End Milling with Application to Cornering Cuts,"; International Journal of Machine Tool Design and Research, Vol. 22, pp. 7-22(1982).
- Pan, W, Ding, S and Mo, J, "The prediction of cutting force in end milling titanium alloy (Ti6Al4V) with polycrystalline diamond tools,"; Proceedings of the Institution of Mechanical Engineers, Part B: Journal of Engineering Manufacture, Vol. 231, no. 1, pp. 3-14(2017).
- Schmitz, T., Mann B., "Closed form solutions for surface location error in milling,"; International Journal of Machine Tools & Manufacture, Vol. 46, pp.1369–77(2006).
- Wang, J.-J. and Zheng, C. M., "Identification of Cutter Axis Offset in End Milling without A Priori Knowledge of Cutting Coefficients,"; International Journal of Machine Tools & Manufacture, Vol. 43, pp. 687-697(2003).
- Wang, J.-J. and Zheng, C. M., "An analytical force model with shearing and ploughing mechanisms for end milling,"; International Journal of Machine Tools & Manufacture, Vol. 42, pp. 761-771(2002).
- Wang, J.-J., Liang, S.Y. and Book, W.J., "Convolution Analysis of Milling Force Pulsation," ; ASME Journal of Engineering for Industry, Vol. 116, pp.17-25(1994).
- Wang, J.-J. and Zheng, C. M., "On-line Identification of Shearing and Plowing Constants in End Milling,"; ASME Journal of Manufacturing Science and Engineering, Vol. 125, pp. 57-64(2003).
- Wang, J.-J. and Zhang, H. C., "Extracting cutting constants via harmonic force components for a general helical end mill,"; Int. J. Adv.

Manuf. Technol., Vol. 24, No. 5, pp. 415–424(2004).

- Yang, M., Park, H., "The prediction of cutting force in ball end milling,"; International Journal of Machine Tools & Manufacture, Vol. 31, pp. 45–54(1991).
- Zhang, S., Li. J.F., Sun, J. J., "Tool wear and cutting forces variation in high speed end-milling Ti-6 Al-4 V alloy,"; Int. J. Adv. Manuf. Technol., Vol. 6, pp. 69–78 (2010).
- Zheng, C. M. and Wang, J.-J., "Stability prediction in radial immersion for milling with symmetric structure,"; International Journal of Machine Tools & Manufacture, Vol. 75, pp. 72-81(2013).
- Zhang , Z., Zheng, L., Zhang, L., Li, Z., Liu, D., and Zhang, B., "A study on calibration of coefficients in end milling forces model,"; Int. J. Adv. Manuf. Technol., Vol.25, Nos.7-8, pp. 652-662(2005).

## APPENDIX

The sum of squared residuals  $S$  is given by

$$S = \left( |A_1'[N]|^2 - |A_1[N]|^2 \right)^2 + \left( |A_2'[N]|^2 - |A_2[N]|^2 \right)^2 \\ = (A_1' - A_1)^2 + (A_2' - A_2)^2. \quad (A1)$$

Minimum  $S$  happens when the gradient  $\frac{\partial S}{\partial k_j}$  ( $j=1, 2$ ) is zero. Since  $S$  contains two parameters  $k_1$  and  $k_2$ , when  $S$  is minimized, two gradient equations can be expressed by

$$\begin{cases} (A_1' - A_1) \frac{\partial A_1}{\partial k_1} + (A_2' - A_2) \frac{\partial A_2}{\partial k_1} = 0 \\ (A_1' - A_1) \frac{\partial A_1}{\partial k_2} + (A_2' - A_2) \frac{\partial A_2}{\partial k_2} = 0 \end{cases}. \quad (A2)$$

In addition, using the truncated Taylor series,  $A_i$  ( $i=1, 2$ ) can be approximated by

$$A_i(\mathbf{k}) \approx A_i(\mathbf{k}^{(n)}) + \sum_{j=1}^2 \frac{\partial A_i(\mathbf{k}^{(n)})}{\partial k_j} (k_j - k_j^{(n)}). \quad (A3)$$

Here,  $n$  is an iteration number, and the initial values of  $\mathbf{k}^{(0)}$  vector can be chosen by substituting  $(k_{rq}, k_{tq})$  into Eq. (18) since  $(k_{rq}, k_{tq})$  are close enough to the desired cutting constants  $(k_{rd}, k_{td})$  in most cutting conditions as mentioned in section 2. After refining  $\mathbf{k}^{(0)}$  iteratively for  $(m-1)$  times, if the difference of norm between the vectors  $\mathbf{k}^{(m)}$  and  $\mathbf{k}^{(m-1)}$  is less than the specified error, the desired  $\mathbf{k}$  can be obtained by

$$\mathbf{k} = \mathbf{k}^{(m)} = \mathbf{k}^{(m-1)} + \Delta \mathbf{k}^{(m-1)} \\ = \begin{pmatrix} k_1^{(m-1)} \\ k_2^{(m-1)} \end{pmatrix} + \begin{pmatrix} k_1^{(m)} - k_1^{(m-1)} \\ k_2^{(m)} - k_2^{(m-1)} \end{pmatrix}. \quad (A4)$$

Substituting Eq. (A3) into Eq. (A2), the shift vector  $\Delta \mathbf{k}^{(m-1)}$  can be found in following matrix

form:

$$\Delta \mathbf{k}^{(m-1)} = (\mathbf{J}_{(m-1)}^T \mathbf{J}_{(m-1)})^{-1} \mathbf{J}_{(m-1)} \Delta \mathbf{A}^{(m-1)}, \quad (A5)$$

where

$$\mathbf{J}_{(m-1)} = \begin{bmatrix} \frac{\partial A_1(\mathbf{k}^{(m-1)})}{\partial k_1} & \frac{\partial A_1(\mathbf{k}^{(m-1)})}{\partial k_2} \\ \frac{\partial A_2(\mathbf{k}^{(m-1)})}{\partial k_1} & \frac{\partial A_2(\mathbf{k}^{(m-1)})}{\partial k_2} \end{bmatrix}, \quad (A6)$$

$$\Delta \mathbf{A}^{(m-1)} = \begin{bmatrix} A'_1 - A_1(\mathbf{k}^{(m-1)}) \\ A'_2 - A_2(\mathbf{k}^{(m-1)}) \end{bmatrix}$$

The subscript  $(m-1)$  of  $\mathbf{J}_{(m-1)}$  and  $\Delta \mathbf{A}^{(m-1)}$  implies that  $\mathbf{J}_{(m-1)}$  and  $\Delta \mathbf{A}^{(m-1)}$  change from one iteration to the next and are associated with  $\mathbf{k}^{(m-1)}$  vector. Once the  $\mathbf{k}^{(m)}$  ( $k_1^{(m)}, k_2^{(m)}$ ) is determined through the iteration analysis, the optimal cutting constants  $k_{td}$  and  $k_{rd}$  are given by

$$\begin{pmatrix} k_{td} \\ k_{rd} \end{pmatrix} = \begin{pmatrix} \frac{2\pi k_1^{(m)}}{N t_x} \\ \frac{k_2^{(m)}}{k_1^{(m)}} \end{pmatrix}. \quad (A7)$$

## NOMENCLATURE

$\alpha, N, R$  helix angle, number of cutter flutes and radius of end mill

$\mathbf{A}$  Fourier series coefficients of the total forces

$\mathbf{A}', A'_x, A'_y$  measured Fourier series coefficients vector of the total forces and its components

$CWD$  chip density function

$d_a, d_r$  axial and radial cutting depths

$\phi$  cutter angular displacement

$\Delta\phi$  phase angle difference between the starting angular position of the force measurement and the origin of cutting position

$\mathbf{k}, \Delta \mathbf{k}$  vector of cutting constants and its shift vector

$k_r, k_t$  cutting constants in radial and tangential directions

$k_{rq}, k_{tq}$  quasi-available cutting constants

$k_{rd}, k_{td}$  optimal cutting constants

$P_1, P_2$  elementary cutting functions of local tangential force

$\theta_1, \theta_2$  entry cutting angle and exit cutting angle

$t_x$  feed per tooth

# 在傳統銑削過程中利用第一諧波分力來估算比切削常數

鄭嘉敏

巴布

福建工程學院機械與汽車工程學院  
司禮文卡特史瓦拉大學工程學院機械工程系

## 摘要

壓電感測器中的電流滲漏經常導致使用動力計的力量信號漂移問題，這問題將導致難以獲得準確的切削力來識別用於連續監測長時間銑削過程的切削常數。為了克服這個困難，本文提出了一種在銑削中的任何時刻僅使用第一諧波分力來辨識切削常數的穩健方法。該方法利用兩個步驟來估算切削常數。第一步是利用測量所得的第一諧波分力的比值中找出切削常數的近似值，第二步是利用最小平方方法根據第一諧波力分力的大小以及步驟一所得的切削常數近似值得來獲得更精確的切削常數。本文還討論了所提方法的局限性並通過銑削實驗證實了該方法的有效性。